DISCLAIMER

This document was prepared as an account of work sponsored by the United States Government. While this document is believed to contain correct information, neither the United States Government nor any agency thereof, nor the Regents of the University of California, nor any of their employees, makes any warranty, express or implied, or assumes any legal responsibility for the accuracy, completeness, or usefulness of any information, apparatus, product, or process disclosed, or represents that its use would not infringe privately owned rights. Reference herein to any specific commercial product, process, or service by its trade name, trademark, manufacturer, or otherwise, does not necessarily constitute or imply its endorsement, recommendation, or favoring by the United States Government or any agency thereof, or the Regents of the University of California. The views and opinions of authors expressed herein do not necessarily state or reflect those of the United States Government or any agency thereof or the Regents of the University of California.

Plasma undulator based on laser excitation of wakefields in a plasma channel

S. G. Rykovanov,* C. B. Schroeder, E. Esarey, C. G. R. Geddes, and W. P. Leemans
Lawrence Berkeley National Laboratory, Berkeley, California 94720, USA
(Dated: March 23, 2015)

An undulator is proposed based on the plasma wakefields excited by a laser pulse in a plasma channel. Generation of the undulator fields is achieved by inducing centroid oscillations of the laser pulse in the channel. The period of such an undulator is proportional to the Rayleigh length of the laser pulse and can be sub-millimeter, while preserving high undulator strength. The electron trajectories in the undulator are examined, expressions for the undulator strength are presented, and the spontaneous radiation is calculated. Multimode and multicolor laser pulses are considered for greater tunability of the undulator period and strength.

Undulator magnets have numerous applications in beam physics, including the production of radiation for light source applications and the cooling of particle beams [1]. The wavelength λ of the radiation produced by an electron undergoing oscillations inside an undulator is $\lambda = \lambda_u \left(1 + K^2/2\right)/2\gamma^2$, where λ_u is the undulator period, γ is the Lorentz factor of the electron, and K is the undulator strength parameter. Presently, the undulator period is limited to >1 mm using conventional magnetic undulators [2]. Reducing λ_u is highly beneficial as it will decrease the required electron energy for the same specified radiation wavelength and, hence, decrease the size of the light source. Undulators with periods less than or on the order of a millimeter, often referred to as micro-undulators, are, therefore, of great interest. Several micro-undulator ideas have been proposed including electro-static undulators [3, 4], crystalline undulators [5], RF-based [6], laser-plasma-based [7–9], and optical undulators [10–17]. In this Letter we propose a micro-undulator based on controlling the transverse forces experienced by an electron beam inside a laser-excited plasma channel. In this concept, a laser injected into a plasma channel excites plasma waves, with the appropriate transverse fields created by laser pulse centroid oscillations in the channel. Together with recent impressive progress in compact laser-plasma electron accelerators (LPAs) [18], this new approach may lead to an extremely compact free-electron laser (FEL).

Plasma channels can be used to guide laser pulses with relativistic intensities (i.e., $I[\mathrm{W/cm^2}] \gtrsim 10^{18}/(\lambda_L[\mu\mathrm{m}])^2$, where I and λ_L are the laser pulse intensity and wavelength, respectively), and laser guiding in plasma channels is routinely used for efficient electron acceleration in LPAs [19–22]. Consider a preformed plasma density profile that is assumed to be parabolic in the direction transverse to the laser propagation

$$n(r) = n_0 \left[1 + (\Delta n/n_0) r^2/w_0^2\right], \tag{1}$$

with r the transverse coordinate, n_0 the on-axis electron density, and Δn the channel depth. For moderate laser intensities, the laser spot size will remain constant during the propagation in such a channel and will be equal to w_0 if the channel depth is equal to $\Delta n = \left(\pi r_e w_0^2\right)^{-1}$, where $r_e = e^2/mc^2$ is the classical electron radius [18]. If the laser pulse enters the channel off-axis or under some angle, the laser beam centroid will oscillate as it propagates, with characteristic oscillation length equal to the Rayleigh range $Z_R = \pi w_0^2/\lambda_L$. For $P < P_c$ and $a_0 < 1$, where P is the laser pulse power, $P_c[\mathrm{GW}] \simeq 17(k_L/k_p)^2$ with $k_L = 2\pi/\lambda_L$ and $k_p = \sqrt{4\pi r_e n_0}$, and $a_0 = eA_L/mc^2$ is the normalized laser vector potential, the laser beam centroid oscillates according to [23, 24]

$$x_c(z) = x_{ci} \cos(z/Z_R + \varphi), \tag{2}$$

where x_{ci} is maximum centroid displacement and is φ an arbitrary phase. Ponderomotively driven plasma waves,

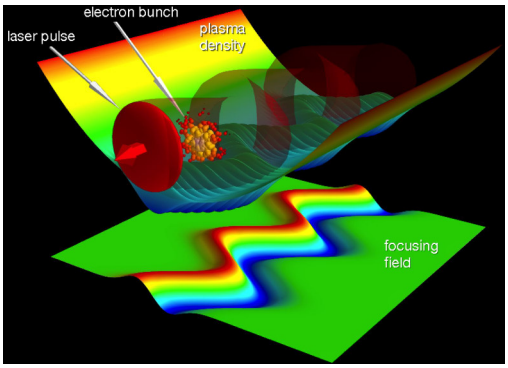

FIG. 1. Schematic of the plasma undulator.

or wakefields, created inside the plasma channel by a short laser pulse with matched spot size and oscillating centroid will follow the laser beam centroid provided $k_p Z_R \gg 1$. As will be shown below, this can be used for controlling the transverse fields of the plasma wave. An electron beam injected in such a *plasma undulator* will experience transverse oscillations leading to efficient radiation generation. An illustration of the plasma undulator is depicted on Fig. 1: A short laser pulse (depicted with red color) is propagating through the plasma channel and exhibits oscillatory centroid motion due to an initial laser centroid displacement. Wakefields created in the plasma also follow the oscillatory laser centroid motion. An electron beam injected behind the laser pulse (depicted by a collection of points) experiences transverse, thus focusing, fields (lower panel) with periodic structure set by the laser centroid oscillation. The periodically-changing focusing field serves as an undulator and the oscillating electrons produce radiation.

We start by deriving the structure of the wakefields excited by the laser pulse undergoing centroid oscillations inside the plasma channel. We assume that the channel is shallow, $k_p w_0 > 1$. We also assume that the laser vector potential amplitude is small $a_0 < 1$, and linear plasma theory can be applied (see, e.g., [18] and references therein). We take the laser pulse profile to be Gaussian in all dimensions (i.e., the laser pulse intensity is proportional to $I \propto \exp\left[-2r^2/w_0^2\right] \exp\left[-2t^2/\tau_L^2\right]$). The plasma is underdense, such that the laser pulse travels through the plasma near the speed of light in vacuum c. In the following, the z-axis is the laser propagation/channel axis. Using linear plasma theory [18], the potential of the laser-excited plasma waves can be expressed as

$$\phi(x,\xi) = -a_0^2 C \sin\left(k_p \xi\right) e^{-2[(x-x_c)^2+y^2]/w_0^2}, \qquad (3)$$

where $\phi = e\Phi/mc^2$ is the normalized scalar potential, $C = \sqrt{\pi/2}(k_p\tau_L/4)\exp(-k_p^2\tau_L^2/8)$ for a linearly-polarized Gaussian laser pulse (for an optimized laser pulse duration $C = \sqrt{\pi/8\mathrm{e}} \approx 0.38$, and $C \to 2C$ for a circularly-polarized laser), $\xi = z - ct$, and x_c is given by Eq. (2). The electric fields, under the assumptions above, are $\boldsymbol{E}/E_0 = -k_p^{-1}\nabla\phi$, where $E_0 = mc^2 k_p/e$, and the equation of motion for an electron in the wakefield is $d(\boldsymbol{p}/mc)/d(k_p ct) = -\boldsymbol{E}/E_0$. We consider injection of the electron beam at a wake phase such that $E_z \simeq 0$. For a single electron, or ultrashort beam, one can consider injection at $\cos(k_p\zeta) = 0$, where $E_z = 0$. For an extended beam one can consider a beam shape and number of electrons that will fully load the wakefield, i.e., cancel the longitudinal wakefield created by the laser pulse with the wakefield created by the electron beam. (Beam loading is discussed below.)

Consider $|x - x_c| \ll w_0$, i.e., the amplitudes of both the laser pulse centroid and electron beam oscillations are small compared to the laser spot size. (Below we discuss the influence of the exponential term in the wakefields on the radiation spectra.) In this limit, the motion of an electron with relativistic gamma factor $\gamma_0 \gg 1$, injected in the phase where $E_z = 0$ and E_x is positive and has the maximum absolute value, is described by a linear harmonically-driven oscillator equation,

$$d^2x/dz^2 + k_\beta^2 x = k_\beta^2 x_{ci} \cos\left(z/Z_R + \varphi\right), \qquad (4)$$

where

$$k_\beta = \left(\frac{4a_0^2 C}{\gamma_0 w_0^2}\right)^{1/2} \qquad (5)$$

is the betatron wavenumber. (The equation of motion in the transverse direction orthogonal to the laser beam centroid motion is $d^2y/dz^2 + k_\beta^2 y = 0$.) The transverse momentum of the electron is

$$p_x/mc = a_{\beta x} \sin\left(k_\beta z + \psi_\beta\right) + a_u \sin\left(k_u z + \varphi\right), \qquad (6)$$

where $k_u = 1/Z_R$, ψ_β is a phase determined by the electron injection relative to the laser beam centroid oscillation,

$$a_{\beta x} = \gamma_0 k_\beta \left| x_m - \frac{(k_\beta Z_R)^2 x_{ci}}{1-(k_\beta Z_R)^2} \right| \qquad (7)$$

$$= \left[\left(\gamma_0 k_\beta x_0 + a_u k_\beta Z_R \cos\varphi\right)^2 + \left(a_u \sin\varphi\right)^2\right]^{1/2} \qquad (8)$$

is the betatron strength parameter, with x_m the maximum transverse displacement of the electron with respect to the channel axis, $x_0 = x(z=0)$ [Eq. (8) assumes $dx(z=0)/dz = 0$], and

$$a_u = \frac{\gamma_0 k_u k_\beta^2 x_{ci}}{k_u^2 - k_\beta^2} \qquad (9)$$

is the undulator strength parameter. The electron is oscillating with two characteristic spatial periods: the betatron motion (with period $2\pi/k_\beta$) and the motion induced by the laser pulse centroid evolution (with period $2\pi Z_R$).

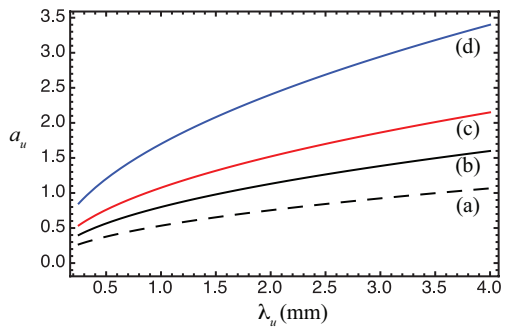

FIG. 2. Undulator strength a_u given by Eq. (11) versus undulator period λ_u for several values of laser amplitude, wavelength, and centroid displacement: (a) $a_0 = 0.28$, $\lambda_L = 1$ μm, and $x_{ci}/w_0 = 0.2$; (b) $a_0 = 0.28$, $\lambda_L = 1$ μm, and $x_{ci}/w_0 = 0.3$; (c) $a_0 = 0.5$, $\lambda_L = 10$ μm, and $x_{ci}/w_0 = 0.4$; and (d) $a_0 = 0.5$, $\lambda_L = 1$ μm, and $x_{ci}/w_0 = 0.2$.

The laser beam centroid oscillations generate undulator motion with the same period

$$\lambda_u = 2\pi^2 w_0^2/\lambda_L. \tag{10}$$

For $k_\beta Z_R \ll 1$, or $2\pi a_0\sqrt{C/\gamma_0} \ll \lambda_L/w_0$, the undulator strength parameters may be approximated as

$$a_u \approx 4\pi a_0^2 C x_{ci}/\lambda_L. \tag{11}$$

The condition $k_\beta Z_R \ll 1$ approximately holds for the parameters considered in this paper. Note that the undulator strength parameter is independent of the electron transverse position. This is in contrast to a simple plasma focusing channel [25], such as that considered by an ion-channel laser [26]. The achievable undulator strength a_u, given by Eq. (11), and λ_u is shown in Fig. 2 for different laser pulse parameters and initial centroid displacements. An undulator strength on the order of unity can be achieved for undulators with mm period.

The properties of the radiation produced by a relativistic electron oscillating in undulator and focusing fields are well-known [1, 2, 27, 28]. Specifically, the n-th harmonic of the normalized undulator radiation wavenumber is

$$\kappa_n = \frac{n\kappa}{1 + a_u^2/2 + a_\beta^2/2 + \gamma_0^2\theta^2}, \tag{12}$$

where $\kappa = k/(2\gamma_0^2 k_u)$ and θ is the azimuthal angle, with $\gamma_0\theta \ll 1$ and $a_\beta^2 = a_{\beta x}^2 + a_{\beta y}^2$. For sufficiently high current and beam quality, partially coherent radiation may be generated by the FEL mechanism [28]. For the FEL instability to grow, beam parameters must be chosen such that $\langle a_\beta^2\rangle/2$ is less than the FEL parameter. For a matched, symmetric beam on-axis, the rms betatron strength parameter is, from Eq. (8),

$$\langle a_\beta^2\rangle = \gamma_0 k_\beta \varepsilon_n + a_u^2\left[(k_\beta Z_R)^2\cos^2\varphi + \sin^2\varphi\right], \tag{13}$$

where ε_n is the normalized emittance of the electron beam. With $k_\beta Z_R < 1$, $\langle a_\beta^2\rangle$ is minimized for $\varphi = 0, \pi$. This plasma undulator configuration is in a strongly focused regime, and for typical LPA beam parameters [18] with ultra-low emittance [29, 30], the beam transverse size will be smaller than the radiation mode size.

Consider the radiation produced by an LPA-generated electron beam propagating through a plasma undulator with the laser-plasma parameters $n_0 = 10^{18}$ cm^{-3}, $\lambda_L = 1$ μm, $w_0 = 7$ μm, $a_0 = 0.28$, and with the laser matched to the plasma channel with centroid oscillation amplitude $x_{ci} = 2.5$ μm. Consider an electron beam phased such that $k_p\zeta = 3\pi/2$ and $\varphi = \pi$, with $\gamma_0 = 1000$ (unless stated otherwise, the rms energy spread of the electron beam is assumed to be $\sigma_\gamma/\gamma_0 = 1\%$). For these parameters, $\lambda_u = 0.97$ mm and $a_u = 1.01$. For the radiation calculation, we have assumed that an electron beam is matched to the focusing forces [25]. Numerical results using VDSR [31] in 2D, with $N_u = 30$ undulator periods and $\varepsilon_n = 0.1$ μm, are summarized in Fig. 3. Figure 3 shows the radiation spectrum $d^2N_{ph}/[N_e(\gamma_0\theta)d(\gamma_0\theta)d\kappa]$, where N_{ph} is the number of photons and N_e is the number of beam electrons, as a function of the normalized wavenumber κ and normalized azimuthal angle $\gamma_0\theta$. Also shown is the on-axis radiation spectrum (solid white line). The peak of the fundamental harmonic of the undulator radiation spectrum is located at $\kappa_1 = (1 + a_u^2/2 + \langle a_\beta^2\rangle/2)^{-1} \approx 0.62$. The harmonics of the undulator radiation given by Eq. (12) are also shown (white dashed curves). Only odd harmonics are generated on-axis, whereas both odd and even harmonics are generated off-axis. The electron beam in the plasma undulator also exhibits betatron oscillations and the peak of the betatron radiation is located at $\kappa_\beta = (k_\beta/k_u)(1 + a_u^2/2 + \langle a_\beta^2\rangle/2)^{-1} \approx 0.15$. The magnitude of betatron radiation is much smaller than the radiation generated at the undulator frequency (since $a_\beta^2 \ll a_u^2$). Note the appearance in Fig. 3 of additional emission at the sum frequencies $\kappa_1 + m\kappa_\beta$, with m a positive integer.

Figure 4 depicts the on-axis radiation spectrum as a function of normalized frequency κ for beams with different values of emittance and energy spread, for the plasma undulator with same parameters as above. Figure 4 shows the on-axis radiation spectrum from an ideal beam (zero emittance and no energy spread) calculated using VDSR (green curve) and using standard undulator radiation theory (dashed black curve) [28]. In Fig. 4, the on-axis radiation spectrum produced by electron beams with $\varepsilon_n = 0.1$ μm (blue curve) and $\varepsilon_n = 0.025$ μm (red curve) are shown. One can see the expected effect of electron beam divergence; the lower the divergence, the narrower the spectrum. Figure 4 also shows (magenta curve) the radiation for a beam with $\varepsilon_n = 0.1$ μm, but with the exponential term in the wakefield included [cf. Eq. (3)]. The spectrum peak is located at higher frequency due to the decrease in the undulator strength. Approximately, the strength of the undulator decreases

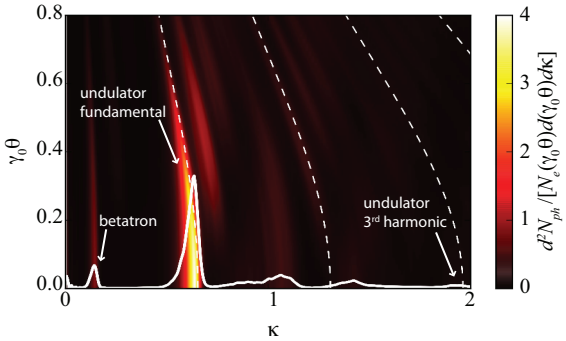

FIG. 3. Normalized radiation spectrum generated by a beam with $\varepsilon_n = 0.1$ μm and $\sigma_\gamma/\gamma_0 = 0.01$, in a plasma undulator with $a_u = 1.01$ and $N_u = 30$. Harmonics, Eq. (12), are shown with white dashed curves. The spectrum for $\theta = 0$ (arb. units) is shown with white solid line. Peaks corresponding to betatron radiation, fundamental and 3rd harmonics of the undulator radiation are annotated with white arrows.

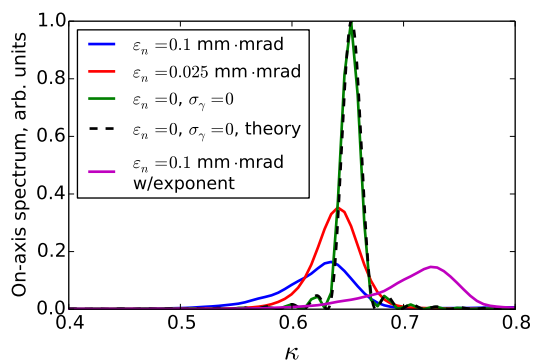

FIG. 4. On-axis spectrum showing the fundamental undulator radiation for several emittance values: $\varepsilon_n = 0.1$ μm (blue curve), $\varepsilon_n = 0.025$ μm (red curve), ideal point-like electron beam with zero emittance and no energy spread [from numerical calculations (green curve) and from theory (dashed black curve)], and $\varepsilon_n = 0.1$ μm with exponential term in the wakefield included (magenta curve). All beams except ideal point-like electron beam case have an energy spread $\sigma_\gamma/\gamma_0 = 1\%$.

by a factor of $\exp(-2x_{ci}^2/w_0^2)$ due to the decrease of the focusing field amplitude off-axis. For the above example, $\exp(-2x_{ci}^2/w_0^2) \approx 0.8$. The decrease in field strength due to the exponential term will depend on the particular situation and can be mitigated by using stronger laser pulses with smaller initial centroid displacements. In the case of the electron bunch with finite emittance and energy spread, the undulator radiation spectrum is broadened compared to the case of a single electron resulting from the beam angular divergence and energy spread.

In our analysis, we have assumed that the electron beam is loaded at the phase where $E_z = 0$ and have neglected the effects due to the longitudinal field E_z. This is valid for the case when longitudinal electron beam size is much smaller than the plasma wavelength (and sufficiently low beam charge) or when a beam of proper shape cancels the longitudinal electric field due to beam loading. Regardless of the beam length, beam loading will limit the amount of charge [32]. The effect of beam loading on the transverse focusing forces of the wake will be small provided that $x_{ci} \gg r_{bm}$, where r_{bm} is the transverse size of the electron beam matched to the wake focusing forces [25]. The effect of the electron beam dephasing can be mitigated by using appropriate plasma density tapering [33].

Additional control of the plasma undulator parameters can also be achieved using the beating of multiple laser pulses with different (odd and even) Hermite-Gaussian modes inside the plasma channel. Plasma wave excitation using multiple laser modes was considered in Ref. [34]. Using the same formalism as above, an electron in the wakefield driven by two linearly-polarized Hermite-Gaussian laser modes will produce undulator and betatron radiation with the parameters:

$$k_{\beta x} = \left(\frac{4C\alpha_x^2}{\gamma_0 w_0^2}\right)^{1/2}, \tag{14}$$

$$k_u = \left|\frac{k_p^2}{2}\left(\frac{1}{k_n} - \frac{1}{k_m}\right) + \frac{(n+1)}{Z_{R,n}} - \frac{(m+1)}{Z_{R,m}}\right|, \tag{15}$$

$$a_u = \frac{C\,|\delta_{n,m}|\,k_u}{w_0(k_u^2 - k_\beta^2)} e^{-(\Delta k)k_p L^2/2} \cosh\left[(\Delta k)k_p L^2\right], \tag{16}$$

with n (even) and m (odd) the mode numbers, $\Delta k = k_n - k_m$, $Z_{R,n}$ and $Z_{R,m}$ are the Rayleigh lengths of two laser pulses [both laser pulses have equal matched radii w_0 and equal rms (intensity) pulse lengths L], and it is assumed $k_n, k_m \gg k_p$. The coefficient α_x^2, assumed to be greater than zero, is

$$\alpha_x^2 = \frac{a_{0,n}^2}{n!2^n}\left[\frac{n!}{(n/2)!}\right]^2 (2n+1) - \frac{4a_{0,m}^2}{m!2^m}\left[\frac{m!}{(\frac{m-1}{2})!}\right]^2, \tag{17}$$

where $a_{0,n}$ and $a_{0,m}$ are the amplitudes of the laser modes (defined in Ref. [34]). Note that, in general, the focusing is asymmetric $k_{\beta x} \neq k_{\beta y}$, however, additional laser pulses, polarized orthogonally (with $\Delta k L \gg 1$) or temporally separated, can be used, following the techniques described in Ref. [34], to control $k_{\beta y}$. The undulator strength is given by the parameter

$$\delta_{n,m} = \frac{4a_{0,n}a_{0,m}}{\sqrt{n!m!2^{n+m-1}}}(-1)^{\frac{n+m-1}{2}} \frac{n!m!}{(\frac{n}{2})!(\frac{m-1}{2})!}. \tag{18}$$

If the mode frequency difference is larger than the plasma frequency, so that $\Delta k \gg k_p \sim 1/L$, then the wake excitation averages over the fast oscillation and $a_u \approx 0$.

For the case when the two laser modes have the same wavelength and considering the modes $n = 0$ and $m = 1$, the undulator period is given by Eq. (10), and, for $k_u \gg k_\beta$, the undulator strength is

$$a_u \approx 2\pi a_{0,0}a_{0,1}Cw_0/\lambda_L. \tag{19}$$

Using multiple modes enables larger undulator strengths (by a factor $\approx w_0/x_{ci}$). Note that a Gaussian laser with a small centroid displacement is equivalent to this case ($k_0 = k_1$): a modal decomposition of a Gaussian with a centroid offset yields $a_{0,0} = a_0$ and $a_{0,1} = a_0 x_{ci}/w_0$, for $x_{ci} \ll w_0$.

The strong focusing of the plasma wave (large a_β) will tend to suppress the FEL instability, since the transverse momentum of each electron will vary with betatron amplitude. As demonstrated in Ref. [34], using multiple Hermite-Gaussian laser modes can reduce the strong focusing of the wakefields (reduce k_β). Consider the following example of a wakefield excited by two laser modes: $n = 0$, $m = 1$, $a_{0,0} = 0.145$, $a_{0,1} = 0.1$, $\lambda_0 = \lambda_1 = 0.8$ μm, and both modes matched to the plasma channel ($n_0 = 10^{18}$ cm^{-3}) with $w_0 = 7$ μm. An injected beam will experience a 1.2 mm undulator period with strength $a_u = 1.2$. Assuming $\gamma_0 = 515$ and $\varepsilon_n = 0.1$ μm, the beam will generate 4 nm radiation. The betatron period is $k_\beta^{-1} \simeq 3.3\lambda_u$ with average betatron strength $\langle a_\beta^2 \rangle \simeq 0.01$ for a matched beam. For 300 A (3 pC in 10 fs), the FEL parameter is $\rho \approx 0.008$.

In conclusion, we have proposed a laser-plasma-based concept for a compact undulator capable of producing sub-millimeter wavelength and undulator strength on the order of unity. Such a plasma undulator is produced by initiating pulse centroid oscillations in a plasma channel or by using multiple laser pulses with different Hermite-Gaussian modes (even and odd). Such a laser-plasma-based undulator offers great flexibility and tunability. For example, polarization control of the plasma undulator is achieved by the direction of the initial laser pulse centroid displacement, and elliptical polarization with arbitrary ellipticity can be produced by injecting the laser pulse into the channel off-axis and at an angle.

This work was supported by supported the Office of Science of the U.S. Department of Energy under Contract No. DE-AC02-05CH11231 and Helmholtz Association (Young Investigator's Group VH-NG-1037). We would like to acknowledge fruitful discussions with M. Zolotorev, C. Benedetti, S. S. Bulanov, and F. Rossi.

* Presently at Helmholtz-Institut Jena, Fröbelstieg 3, 07743, Jena, Germany.

[1] A. W. Chao, K. H. Mess, M. Tigner, and F. Zimmermann, eds., *Handbook of Accelerator Physics and Engineering*, 2nd ed. (World Scientific, 2013).
[2] J. Clarke, *The Science and Technology of Undulators and Wigglers* (Oxford University Press, 2004).
[3] R. Tatchyn, Rev. Mod. Phys. **60**, 2571 (1989).
[4] V. Papadichev, Nucl. Instrum. Methods Phys. Res. A **429**, 377 (1999).
[5] S. Bellucci, S. Bini, V. M. Biryukov, Y. A. Chesnokov, S. Dabagov, G. Giannini, V. Guidi, Y. M. Ivanov, V. I. Kotov, V. A. Maisheev, C. Malagù, G. Martinelli, A. A. Petrunin, V. V. Skorobogatov, M. Stefancich, and D. Vincenzi, Phys. Rev. Lett. **90**, 034801 (2003).
[6] S. Tantawi, M. Shumail, J. Neilson, G. Bowden, C. Chang, E. Hemsing, and M. Dunning, Phys. Rev. Lett. **112**, 164802 (2014).
[7] C. Joshi, T. Katsouleas, J. M. Dawson, Y. T. Yan, and J. M. Slater, IEEE J. Quantum Electron. **QE-23**, 1571 (1987).
[8] S. Corde and K. Ta Phuoc, Phys. Plasmas **18**, 033111 (2011).
[9] I. Andriyash, R. Lehe, A. Lifschitz, C. Thaury, J.-M. Rax, K. Krushelnick, and V. Malka, Nature Communications **5**, 4736 (2014).
[10] P. Sprangle and E. Esarey, Phys. Fluids B **4**, 2241 (1992).
[11] P. Sprangle, A. Ting, E. Esarey, and A. Fisher, J. Appl. Phys. **72**, 5032 (1992).
[12] M. Zolotorev, Nucl. Instrum. Methods Phys. Res. A **483**, 445 (2002).
[13] P. Sprangle, B. Hafizi, and J. R. Peñano, Phys. Rev. ST Accel. Beams **12**, 050702 (2009).
[14] A. Bacci, M. Ferrario, C. Maroli, V. Petrillo, and L. Serafini, Phys. Rev. ST Accel. Beams **9**, 060704 (2006).
[15] A. D. Debus, M. Bussmann, M. Siebold, A. Jochmann, U. Schramm, T. E. Cowan, and R. Sauerbrey, Appl. Phys. B **100**, 61 (2010).
[16] J. E. Lawler, J. Bisognano, R. A. Bosch, T. C. Chiang, M. A. Green, K. Jacobs, T. Miller, R. Wehlitz, D. Yavuz, and R. C. York, J. Phys. D: Appl. Phy. **46**, 325501 (2013).
[17] C. Chang, C. Tang, and J. Wu, Phys. Rev. Lett. **110**, 064802 (2013).
[18] E. Esarey, C. Schroeder, and W. Leemans, Rev. Mod. Phys. **81**, 1229 (2009).
[19] C. G. R. Geddes, C. Toth, J. van Tilborg, E. Esarey, C. B. Schroeder, J. Cary, and W. P. Leemans, Phys. Rev. Lett. **95**, 145002 (2005).
[20] W. P. Leemans, B. Nagler, A. J. Gonsalves, C. Tóth, K. Nakamura, C. G. R. Geddes, E. Esarey, C. B. Schroeder, and S. M. Hooker, Nature Phys. **2**, 696 (2006).
[21] T. P. A. Ibbotson, N. Bourgeois, T. P. Rowlands-Rees, L. S. Caballero, S. I. Bajlekov, P. A. Walker, S. Kneip, S. P. D. Mangles, S. R. Nagel, C. A. J. Palmer, N. Delerue, G. Doucas, D. Urner, O. Chekhlov, R. J. Clarke, E. Divall, K. Ertel, P. S. Foster, S. J. Hawkes, C. J. Hooker, B. Parry, P. P. Rajeev, M. J. V. Streeter, and S. M. Hooker, Phys. Rev. ST Accel. Beams **13**, 031301 (2010).
[22] W. P. Leemans, A. J. Gonsalves, H.-S. Mao, K. Nakamura, C. Benedetti, C. B. Schroeder, C. Tóth, J. Daniels, D. E. Mittelberger, S. S. Bulanov, J.-L. Vay, C. G. R. Geddes, and E. Esarey, Phys. Rev. Lett. **113**, 245002 (2014).
[23] P. Sprangle, J. Krall, and E. Esarey, Phys. Rev. Lett. **73**, 3544 (1994).
[24] A. J. Gonsalves, K. Nakamura, C. Lin, J. Osterhoff, S. Shiraishi, C. B. Schroeder, C. G. R. Geddes, C. Tóth, E. Esarey, and W. P. Leemans, Phys. Plasmas **17**, 056706 (2010).
[25] E. Esarey, B. A. Shadwick, P. Catravas, and W. P. Leemans, Phys. Rev. E **65**, 056505 (2002).
[26] D. H. Whittum, A. M. Sessler, and J. M. Dawson, Phys. Rev. Lett. **64**, 2511 (1990).
[27] D. Attwood, *Soft X-Rays and Extreme Ultraviolet Radi-*

ation (Cambridge University Press, 1999).

[28] P. Schmueser, M. Dohlus, and J. Rossbach, *Ultraviolet and Soft X-Ray Free-Electron Lasers: Introduction to Physical Principles, Experimental Results, Technological Challenges* (Springer, 2008).

[29] G. R. Plateau, C. G. R. Geddes, D. B. Thorn, M. Chen, C. Benedetti, E. Esarey, A. J. Gonsalves, N. H. Matlis, K. Nakamura, C. B. Schroeder, S. Shiraishi, T. Sokollik, J. van Tilborg, Cs. Tóth, S. Trotsenko, T. S. Kim, M. Battaglia, T. Stöhlker, and W. P. Leemans, Phys. Rev. Lett. **109**, 064802 (2012).

[30] R. Weingartner, S. Raith, A. Popp, S. Chou, J. Wenz, K. Khrennikov, M. Heigoldt, A. R. Maier, N. Kajumba, M. Fuchs, B. Zeitler, F. Krausz, S. Karsch, and F. Grüner, Phys. Rev. ST Accel. Beams **15**, 111302 (2012).

[31] M. Chen, E. Esarey, C. G. R. Geddes, C. B. Schroeder, G. R. Plateau, S. S. Bulanov, S. Rykovanov, and W. P. Leemans, Phys. Rev. ST Accel. Beams **16**, 030701 (2013).

[32] T. Katsouleas, S. Wilks, P. Chen, J. M. Dawson, and J. J. Su, Part. Accel. **22**, 81 (1987).

[33] W. Rittershofer, C. B. Schroeder, E. Esarey, F. J. Grüner, and W. P. Leemans, Phys. Plasmas **17**, 063104 (2010).

[34] E. Cormier-Michel, E. Esarey, C. G. R. Geddes, C. B. Schroeder, K. Paul, P. J. Mullowney, J. R. Cary, and W. P. Leemans, Phys. Rev. ST Accel. Beams **14**, 031303 (2011).